Iranian Journal of
Numerical Analysis and Optimization

Ferdowsi University of Mashhad

Reaserch Article

Mathematical modeling and optimal control of hepatitis B virus dynamics

L. El Houari, M. Elkaf and J. Danane

DOI:10.22067/ijnao.2026.97045.1806

Vol. 17, No. 1, March 2027

pp. 273–289

Ferdowsi University of Mashhad, Iran

Iranian Journal of Numerical Analysis and Optimization
Vol. 17, No. 1, 2027, pp 273–289
https://doi.org/10.22067/ijnao.2026.97045.1806
https://ijnao.um.ac.ir/

CC BY NC

Research Article

Mathematical modeling and optimal control of hepatitis B virus dynamics

L. El Houari*, M. Elkaf and J. Danane

Abstract

In this study, we examine the dynamics of Hepatitis B Virus, formulated through a system of four differential equations that describe the interactions between healthy hepatocytes, infected hepatocytes, capsids, and HBV. To establish the well-posedness of the proposed model, we prove the positivity and boundedness of solutions under two control strategies. Then, we give some numerical results confirming that control strategies play a crucial role in reducing viral load, leading to improved disease management and prevention of complications such as liver damage. The overall findings emphasize the importance of intervention in maintaining biological balance and enhancing health outcomes.

AMS subject classifications (2020): Primary 92C50, 49J15; Secondary 34A34, 34D20, 65L06, 37N25.

*Corresponding author

Received 17 December 2025; revised 3 July 2026; accepted 8 August 2026

Loubna El Houari
LaMAO Laboratory, Faculty of Sciences, Mohammed First University, Oujda, Morocco. e-mail: l.elhouari@ump.ac.ma.

Mariem Elkaf
Royal Naval School, Casablanca, Morocco. e-mail: elkaf.mariem@gmail.com.

Jaouad Danane
National School of Applied Sciences, Hassan First University, Berrechid, Morocco. e-mail: jaouad-danane@gmail.com

How to cite this article
El Houari, L., Elkaf, M. and Danane, J., Mathematical modeling and optimal control of hepatitis B virus dynamics. *Iran. J. Numer. Anal. Optim.*, 2027; 17(1): 273-289. https://doi.org/10.22067/ijnao.2026.97045.1806

Keywords: HBV, Dynamical system, Ordinary differential equations, Stability, optimal control, Optimization, Numerical simulation.

1 Introduction

The hepatitis B virus (HBV) is a pathogen known to cause serious liver disease by infecting healthy hepatocytes. This condition is highly contagious and can spread through contact with infected bodily fluids [7, 16]. Due to its ease of transmission, HBV infection represents a major global health concern. According to estimates from the World Health Organization (WHO), hepatitis B and C lead to approximately one million deaths annually, with around three million new infections reported each year [19, 20].

To gain a deeper understanding of the dynamics behind hepatitis B viral infection, numerous mathematical models have been developed, introducing the capsid as an element in the dynamics of HBV disease to show that optimized drug treatments can reduce viral load and increase healthy cells [9, 8, 14]. These models aim to study and predict the virus's behavior and progression. It is well known that infected liver cells release HBV DNA-containing capsids in the form of mature viruses [17, 12, 11]. A significant body of research has focused on optimizing the control of HBV infection by targeting these capsids [6, 13], showing that optimal therapy effectively controls viral replication and improves treatment outcomes. Furthermore, other studies have explored this infection through different mathematical frameworks, including fractional differential equations (FDEs) [18, 1, 2, 5], ordinary differential equations (ODEs) [17, 6, 11], and partial differential equations (PDEs) [4, 10].

More recent investigations [16, 9, 14] have incorporated the capsid parameter into their models, examining aspects such as stability and optimal control strategies. These numerous contributions highlight the crucial role that mathematical modeling plays in enhancing our understanding of the HBV infection process.

Based on a comprehensive review and critical analysis of previous research [11, 15], we propose the following model that consists of four variables describing the dynamics of HBV infection. The problem is formulated as a nonlinear differential system:

$$\begin{cases} \frac{dH}{dt} = s - \mu H - k\frac{HV}{H+I}, \\ \frac{dI}{dt} = k\frac{HV}{H+I} - \delta I, \\ \frac{dD}{dt} = aI - (\beta+\delta)D, \\ \frac{dV}{dt} = \beta D - uV. \end{cases} \tag{1}$$

The variables of our model are as follows:

- (H) Healthy hepatocyte cells,
- (I) Infected cells,
- (D) Capsids,
- (V) Hepatitis B virus.

They vary as follows:

- The hepatocytes (H) are produced at a rate of s and die at a rate of μ. These healthy cells become infected by the virus at a rate of $k\frac{HV}{H+I}$, where k is the infection rate.
- The infected cells (I) arise from the infection of healthy hepatocytes at a rate of $k\frac{HV}{H+I}$ and naturally die at a rate of δ.
- The capsids (D) are produced at a rate of a, transmitted to the blood at a rate of β, and decay at a rate of δ.
- The virus (V) grows in the bloodstream at a rate of β due to DNA-containing capsids and decays at a rate of u.

The parameters of model (1), along with their corresponding units and values, are grouped in Table 1.

To provide clearer insight into this formulation of HBV infection dynamics, we present Figure 1, which illustrates the viral progression and models the various interactions among the variables.

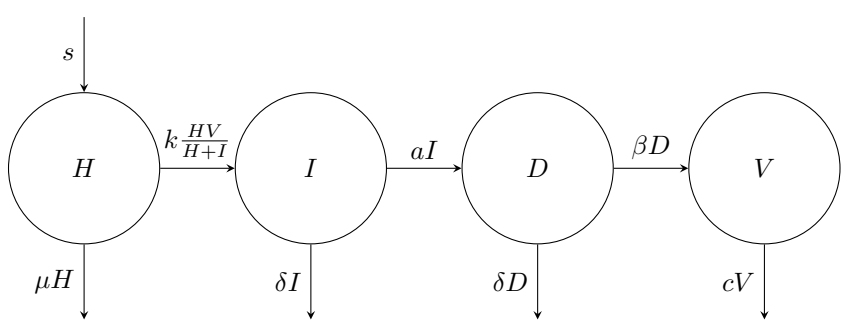

Figure 1: A graphical diagram illustrating the dynamics of HBV.

However, certain therapies or drugs can reduce HBV infection, highlighting the importance of studying the impact of optimal therapeutic control on HBV viral dynamics. For this purpose, we denote α_1 and α_2 as the efficacy rates of drugs or therapies 1 and 2, respectively. Thus, the model becomes

$$\begin{cases} \frac{dH}{dt} = s - \mu H - k(1-\alpha_1)\frac{HV}{H+I}, \\ \frac{dI}{dt} = k(1-\alpha_1)\frac{HV}{H+I} - \delta I, \\ \frac{dD}{dt} = a(1-\alpha_2)I - (\beta+\delta)D, \\ \frac{dV}{dt} = \beta D - uV. \end{cases} \tag{2}$$

Remark 1. The efficacy values of drugs or therapies range between 0 and 1.

The manuscript is organized into several sections. In Section 2, we focus on the stability criterion of the model. Section 3 addresses the model's optimization analysis as previously employed in [3]. In Section 4, we develop a numerical algorithm and present several numerical simulations. Finally, we summarize our findings and discuss future perspectives in the conclusion Section 5.

2 Optimization criterion

In the present section, we analyze the well-posedness of the HBV dynamics model by ensuring the positivity and boundedness of solutions, thereby preserving the biological relevance of the infection model. We also determine the disease's steady states and then examine the threshold for effective therapy.

2.1 Positivity and boundedness

We assume that the initial conditions of the solutions are positive to maintain biological relevance. In this subsection, we show the well-posedness of the solution to model (2).

Theorem 1. The solutions of the given problem in (2) are bounded and nonnegative.

Proof. Indeed, for $(H(t), I(t), D(t), V(t)) \in \mathbb{R}^4_+$, we have

$\frac{dH}{dt}\big|_{H=0} = s \geq 0,$

$\frac{dI}{dt}\big|_{I=0} = k(1-\alpha_1)V \geq 0,$

$\frac{dD}{dt}\big|_{D=0} = a(1-\alpha_2)I \geq 0,$

$\frac{dV}{dt}\big|_{V=0} = \beta D \geq 0.$

Therefore, all solutions initiating in $\mathbb{R}^4_+$ are positive, which shows the nonnegativity of the solution.

To demonstrate that the solutions remain bounded, we obtain the following inequalities from the equations of model (2):

$\frac{dH}{dt} + \mu H \leq s,$
$\frac{d(H+I)}{dt} + \mu_1(H+I) \leq s,$ where we set $\mu_1 = \min(\mu, \delta)$,
$\frac{dD}{dt} + (\beta+\delta)D \leq a(1-\alpha_2)I,$
$\frac{dV}{dt} + uV \leq \beta D.$
Thus
$H \leq \left(H_0 - \frac{s}{\mu}\right) e^{-\mu t} + \frac{s}{\mu},$
$H + I \leq \left(H_0 + I_0 - \frac{s}{\mu_1}\right) e^{-\mu_1 t} + \frac{s}{\mu_1}.$
We deduce the boundedness of H. Since H is bounded, I is also bounded.
Thus
$D \leq D_0 e^{-(\beta+\delta)t} + \int_0^t a(1-\alpha_2) I e^{-(\beta+\delta)(t-\zeta)} d\zeta.$
Since I is bounded, D is also bounded.
Thus
$V \leq V_0 e^{-ut} + \int_0^t \beta D e^{-u(t-\zeta)} d\zeta.$
Since D is bounded, V is also bounded. □

2.2 Steady states

Before examining the stability of the viral dynamics, we must calculate the basic reproduction number (BRN). This value represents the average number of new cases generated by a single infected cell. Mathematically, it is defined as the spectral radius of the next-generation matrix.

Using the dominant eigenvalue, we obtain the following calculation results, allowing us to express R_0 as follows:

$$R_0 = \frac{k(1-\alpha_1)(1-\alpha_2)a\beta}{\delta u(\beta+\delta)}.$$

We seek to determine all possible equilibrium points. Simple calculations show that there is one disease-free equilibrium $E_f(\frac{s}{\mu}, 0, 0, 0)$. Furthermore, we can find an endemic steady state $E_e(H_e, I_e, D_e, V_e)$ when

$H_e = \frac{s}{\delta(R_0-1)+\mu}$,
$I_e = \frac{s(R_0-1)}{\delta(R_0-1)+\mu}$,
$D_e = \frac{a(1-\alpha_2)s(R_0-1)}{(\beta+\delta)(\delta(R_0-1)+\mu)}$,
$V_e = \frac{\beta a(1-\alpha_2)s(R_0-1)}{u(\beta+\delta)(\delta(R_0-1)+\mu)}$.

Remark 2. We observe that the endemic equilibrium point exists when R_0 is greater than one.

Theorem 2. The disease-free equilibrium point E_f is locally stable when $R_0 < 1$.

The endemic equilibrium point E_e exists and is locally stable when $R_0 \geq 1$.

Proof. We compute the Jacobian matrix of system (2) at the equilibrium points and discuss the signs of its eigenvalues. **Stability of the disease-free equilibrium E_f:**
The Jacobian matrix at $E_f = \left(\frac{s}{\mu}, 0, 0, 0\right)$ is

$$J(E_f) = \begin{pmatrix} -\mu & 0 & 0 & -k \\ 0 & -\delta & 0 & k \\ 0 & a & -(\beta+\delta) & 0 \\ 0 & 0 & \beta & -u \end{pmatrix}.$$

Its characteristic polynomial is

$$P_{E_f}(\lambda) = (\mu+\lambda)(\delta+\lambda)\left[(\beta+\delta+\lambda)(u+\lambda) - ak\beta\right].$$

The first two eigenvalues are clearly negative. The rest of the roots have negative real parts if and only if

$$(\beta+\delta)u - ak\beta > 0,$$

which is equivalent to

$$R_0 < 1.$$

Hence, E_f is locally asymptotically stable when $R_0 < 1$.
Stability of the endemic equilibrium E_e:
For $R_0 \geq 1$, the equilibrium $E_e(H_e, I_e, D_e, V_e)$ exists.
The Jacobian matrix at $E_e = (H_e, I_e, D_e, V_e)$ is

$$J(E_e) = \begin{pmatrix} -\mu - k\frac{V_e I_e}{(H_e+I_e)^2} - k\frac{V_e}{H_e+I_e} & -k\frac{H_e V_e}{(H_e+I_e)^2} & 0 & -k\frac{H_e}{H_e+I_e} \\ k\frac{V_e I_e}{(H_e+I_e)^2} + k\frac{V_e}{H_e+I_e} & k\frac{H_e V_e}{(H_e+I_e)^2} - \delta & 0 & k\frac{H_e}{H_e+I_e} \\ 0 & a & -(\beta+\delta) & 0 \\ 0 & 0 & \beta & -u \end{pmatrix}.$$

Its characteristic polynomial is

$$P(\lambda) = \left[(\lambda - a_{11})(\lambda - a_{22}) - a_{12}a_{21}\right](\lambda + \beta + \delta)(\lambda + u),$$

where
$a_{11} = -\mu - k\frac{V_e I_e}{(H_e+I_e)^2} - k\frac{V_e}{H_e+I_e}$,
$a_{22} = k\frac{H_e V_e}{(H_e+I_e)^2} - \delta$,
$a_{12} = -k\frac{H_e V_e}{(H_e+I_e)^2}$,
and $a_{21} = k\frac{V_e I_e}{(H_e+I_e)^2} + k\frac{V_e}{H_e+I_e}$.

The first two eigenvalues are clearly negative. The rest of the roots have negative real parts if and only if

$$-a_{11} - a_{22} > 0 \quad \text{and} \quad a_{11}a_{22} - a_{12}a_{21} > 0,$$

which is always true under the hypothesis $\delta \geq \mu$. Therefore, all eigenvalues of $J(E_e)$ have negative real parts, and the endemic equilibrium is locally asymptotically stable when $R_0 \geq 1$. □

2.3 Critical therapy efficacy

In system (2), the effectiveness of drugs 1 and 2 is represented by the terms $1 - \alpha_1$ and $1 - \alpha_2$, respectively. Thus, the values $\alpha_i = 0$ and $\alpha_i = 1$ (for $i = 1, 2$) indicate complete ineffectiveness and full effectiveness of the respective drug. For simplicity, we combine the effectiveness of both drugs into a single term that reflects overall efficacy: $1 - \eta = (1 - \alpha_1)(1 - \alpha_2)$.

The new BRN becomes

$$R_0 = \frac{k(1-\eta)a\beta}{\delta u(\beta+\delta)}.$$

To determine the critical drug and therapy efficacy η_{crit}, we set $R_0 = 1$.

Thus,

$$\eta_{\text{crit}} = 1 - \frac{\delta u(\beta+\delta)}{ka\beta}.$$

Therefore, for a comprehensive interpretation, if $\eta \leq \eta_{\text{crit}}$ $(R_0 \geq 1)$, then the HBV infection will continue to persist.

Conversely, if $\eta > \eta_{\text{crit}}$ $(R_0 < 1)$, then this suggests disease elimination.

3 Optimal control techniques

We formulate the optimal control problem by introducing the cost functional J, defined by the following expression:

$$J(\alpha_1, \alpha_2) = \frac{1}{2} \int_0^{t_f} \left\{ Q_1 \alpha_1^2(t) + Q_2 \alpha_2^2(t) + Q_3 V^2(t) + Q_4 D^2(t) \right\} dt, \tag{3}$$

where t_f denotes the duration of the treatment. The positive constants Q_1, Q_2, Q_3, and Q_4 represent the benefit-cost weights associated with the control functions α_1 and α_2, respectively. The control functions $\alpha_1(t)$ and $\alpha_2(t)$ are assumed to be bounded and Lebesgue integrable over the time interval $[0, t_f]$. The aim is to minimize the objective functional defined in (3) by simultaneously reducing the number of infected cells, lowering the viral load, and minimizing the cost associated with treatment. In this context, we construct the Hamiltonian associated with the optimal control problem in order to derive the necessary optimality conditions.

More precisely, for the state vector $x(t) = (H, I, D, V)$, where H, I, D, and V denote the healthy cells, infected cells, capsids, and virus, respectively, the Hamiltonian is given by

$$\mathcal{H} = \frac{1}{2}(Q_1 \alpha_1^2 + Q_2 \alpha_2^2 + Q_3 V^2 + Q_4 D^2) + \lambda_1 \frac{\partial H}{\partial t} + \lambda_2 \frac{\partial I}{\partial t} + \lambda_3 \frac{\partial D}{\partial t} + \lambda_4 \frac{\partial V}{\partial t}. \tag{4}$$

The Hamiltonian combines the objective functional with the state equations through the adjoint variables. The we seek an optimal control pair

$$(\alpha_1^*, \alpha_2^*) = \underset{U}{argmin}\, \mathcal{H}(x^*, \alpha_1, \alpha_2, \lambda_1, \lambda_2, \lambda_3, \lambda_4, t) \tag{5}$$

that achieves the desired therapeutic outcomes in an efficient and cost-effective manner.
The functional $\mathcal{H}$ is Fréchet differentiable with respect to its arguments. Moreover, we assume that $(\alpha_1, \alpha_2) \in U$, where U denotes the control set defined by

$$\begin{aligned} U = \{ &(\alpha_1(t), \alpha_2(t)) \text{ such that } \alpha_1(t), \alpha_2(t) \text{ are measurable} \\ &\text{and satisfy } 0 \leq \alpha_i(t) \leq 1, t \in [t_0, t_f], \text{ for } i = 1, 2\}. \end{aligned} \tag{6}$$

For a minimization problem, Pontryagin's maximum principle gives the condition:

$$\mathcal{H}(x^*, \alpha_1^*, \alpha_2^*, \lambda_1^*, \lambda_2^*, \lambda_3^*, \lambda_4^*, t) = 0. \tag{7}$$

This means that, for fixed $x^*(t), \lambda_1(t), \lambda_2(t), \lambda_3(t), \lambda_4(t)$, and t, the function $x \to \mathcal{H}(x^*, \lambda_1, \lambda_2, \lambda_3, \lambda_4)$ must attain its minimum on the admissible control set U.

3.1 Existence and uniqueness of an optimal control pair

The discussion of the existence, uniqueness, and characterization of the optimal control pair is presented in this section by proving that the Hamiltonian $\mathcal{H}$ admits a unique minimum with respect to the control variable.

The results are established using the following lemmas.

Lemma 1. The functional $\mathcal{H}$ defined in (4) is continuous, strictly convex on the set U, and satisfies

$$\lim_{\|(\alpha_1,\alpha_2)\| \to +\infty} \mathcal{H}(\alpha_1, \alpha_2) = +\infty.$$

Proof. Since it is bounded from below by a quadratic function that goes to infinity, $\mathcal{H}$ tends to ∞, clearly satisfying the properties outlined in Lemma 1 on the set U. Moreover, $\mathcal{H}$ is strictly convex because its second derivative is positive. □

Lemma 2. It holds that U defined in (6) is a nonempty, closed, and convex subset of $L^2([t_0, t_f])$.

Proof. By the definition, the set U of admissible controls and associated state variables is a nonempty, convex, and closed subset. □

In this subsection, we have shown that the functional $\mathcal{H}$ is continuous, strictly convex on the set U, and satisfies

$$\lim_{\|(\alpha_1,\alpha_2)\| \to +\infty} \mathcal{H}(\alpha_1, \alpha_2) = +\infty,$$

where U is a nonempty, convex, and closed set. As a result, we conclude that the functional $\mathcal{H}$ admits a unique minimum (α_1^*, α_2^*).

3.2 Derivation of adjoint equations

The adjoint equations are obtained by differentiating the Hamiltonian with respect to the state variables. More precisely, for each state variable $x_i(t)$, the corresponding adjoint variable $\lambda_i(t)$

satisfies

$$\begin{aligned}
\dot{\lambda}_1 &= \frac{d\lambda_1}{dt} = -\frac{\partial \mathcal{H}}{\partial H} = \lambda_1\mu + (\lambda_1 - \lambda_2)k(1-\alpha_1)\frac{VI}{(H+I)^2}, \\
\dot{\lambda}_2 &= \frac{d\lambda_2}{dt} = -\frac{\partial \mathcal{H}}{\partial I} = (\lambda_2 - \lambda_1)(1-\alpha_1)\frac{kHV}{(H+I)^2} + \lambda_2\delta - a(1-\alpha_2)\lambda_3, \\
\dot{\lambda}_3 &= \frac{d\lambda_3}{dt} = -\frac{\partial \mathcal{H}}{\partial D} = \lambda_3(\beta+\delta) - \lambda_4\beta - Q_4 D, \\
\dot{\lambda}_4 &= \frac{d\lambda_4}{dt} = -\frac{\partial \mathcal{H}}{\partial V} = (\lambda_1 - \lambda_2)k(1-\alpha_1)\frac{H}{H+I} + \lambda_4\mu - Q_3 V,
\end{aligned} \tag{8}$$

with $\lambda_1(t_f) = \lambda_2(t_f) = \lambda_3(t_f) = \lambda_4(t_f) = 0$

3.3 Optimality conditions

Assuming that (α_1^*, α_2^*) is an optimal control pair minimizing the Hamiltonian $\mathcal{H}$, we derive below the optimality conditions corresponding to problem (5).

Theorem 3. There exists a unique optimal control pair (α_1^*, α_2^*) that solves the optimization problem (4) such that the gradient of the Hamiltonian $\mathcal{H}$ satisfies the following optimality condition:

$$\begin{aligned}
\alpha_1^* &= (\lambda_2 - \lambda_1)\frac{kHV}{(H+I)Q_1}, \\
\alpha_2^* &= \frac{\lambda_3 a I}{Q_2}.
\end{aligned}$$

Proof. Let us assume that (α_1^*, α_2^*) is an optimal control pair minimizing the Hamiltonian $\mathcal{H}$. The optimality is characterized by the first-order necessary condition:

$$\frac{\partial \mathcal{H}}{\partial \alpha_1} = Q_1\alpha_1 + (\lambda_1 - \lambda_2)\frac{kHV}{H+I} = 0,$$

$$\frac{\partial \mathcal{H}}{\partial \alpha_2} = Q_2\alpha_2 - \lambda_3 a I = 0.$$

That is,

$$\alpha_1^* = (\lambda_2 - \lambda_1)\frac{kHV}{(H+I)Q_1},$$

$$\alpha_2^* = \frac{\lambda_3 a I}{Q_2}.$$

□

4 Numerical section

This section is devoted to presenting numerical simulations that illustrate the theoretical results derived in the previous section.

4.1 Iterative algorithm

The optimization problem (5) can be solved using a descent method described by the following algorithm.

1. Select an initial pair (α_1^0, α_2^0);

2. Solve state equations (2) forward in time using implicit Euler method.

3. Solve adjoint equations (8) backward in time using implicit Euler method.

4. Update the controls using the optimality condition, that is, $(\alpha_1^{n+1}, \alpha_2^{n+1}) = (\alpha_1^n, \alpha_2^n) - m_n d_n$, where d_n is the search direction. The search direction d_n is computed depending on the applied optimization technique. Herein, we use $d_n = \nabla \mathcal{H}$,
   Also, m_n (step size) is chosen by using the Armijo rule.

5. The stopping criterion for the minimization process is defined by

$$\|\nabla \mathcal{H}\| < \varepsilon,$$

   where ε is a prescribed convergence parameter.

4.2 Numerical simulations

To solve the system (2) numerically, we use the previous algorithm. Table 1 describes the parameter values used for the simulations [8, 14].

Table 1: Parameter description of system (1)

Parameters	Descriptions	Units	Values
s	Production rate of healthy hepatocytes	cells.mm^{-3}.day^{-1}	2.6×10^7
μ	Natural death rate of healthy hepatocytes	day^{-1}	0.01
k	Infection rate of healthy cells by the virus	cells.virion^{-1}.day^{-1}	3×10^{-4}
δ	Natural death rate of infected cells and capsids	day^{-1}	0.053
a	Production rate of capsids by infected cells	day^{-1}	150
β	Rate at which capsids are converted into virus	day^{-1}	0.87
u	Decay rate of free virus	day^{-1}	3.8

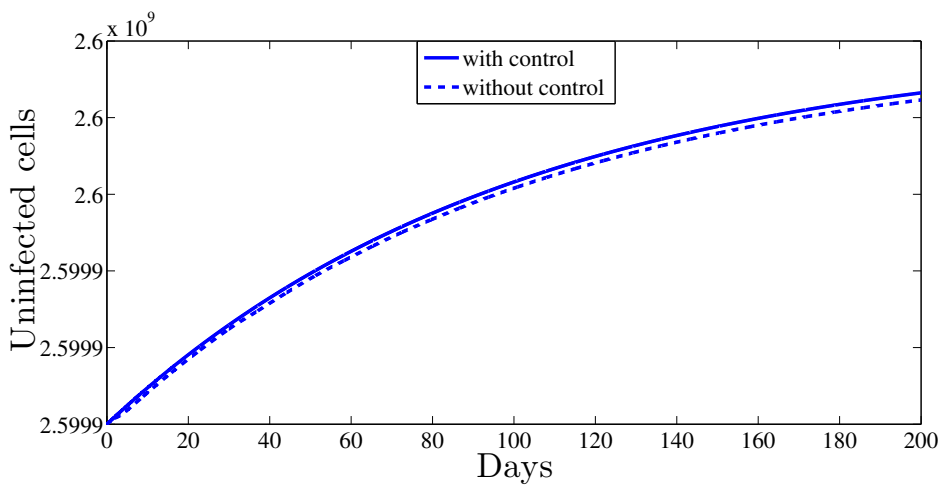

Figure 2: The effect of the control strategy on uninfected hepatocytes

Figure 2 illustrates the dynamics of uninfected hepatocytes over a period of 200 days. A solid blue line in the plot indicates a scenario with therapeutic control, while a dashed blue line indicates a situation without control. The results indicate that the presence of a control strategy leads to a slightly higher number of uninfected hepatocytes over time, suggesting that therapeutic intervention contributes to the preservation of healthy liver cells.

The dynamics of infected hepatocytes throughout time are shown in Figure 3. The number of infected cells is high at first but quickly drops, especially when a control mechanism is in place. Two situations are contrasted in the plot: One with control (solid line) and the other without

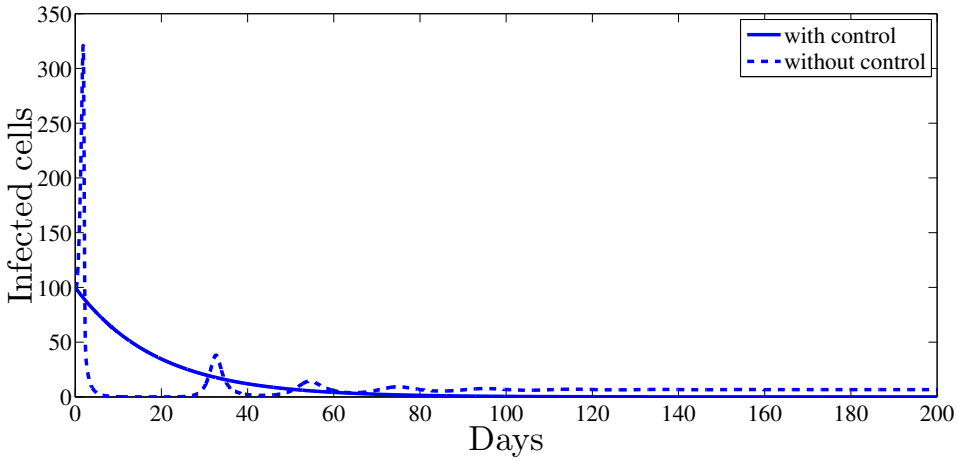

Figure 3: The effect of the control strategy on infected hepatocytes

(dashed line). The outcomes demonstrate the therapeutic efficacy of the control technique by showing that it considerably lowers the number of infected hepatocytes more efficiently than in the uncontrolled scenario.

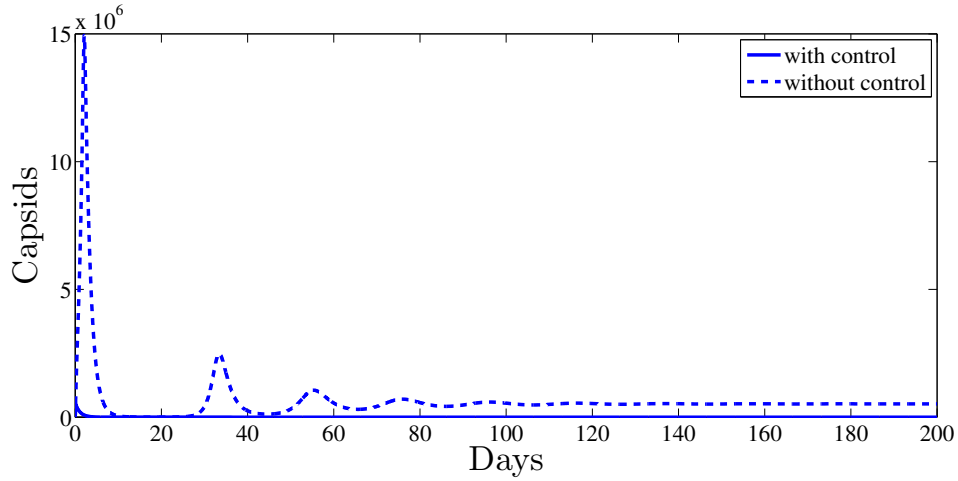

Figure 4: The effect of the control strategy on Capsids

Figure 4 compares the levels of capsids over a 200-day period under two conditions: with control and without control. It likely demonstrates that the control strategy effectively reduces or stabilizes capsid levels over time, in contrast to the uncontrolled condition where capsid levels may rise or persist. The line with control would show a decline or stabilization in capsid levels, while the line without control might indicate higher or increasing levels. This suggests that the

control strategy plays an important role in managing capsid levels, which is critical in fields like virology and drug development.

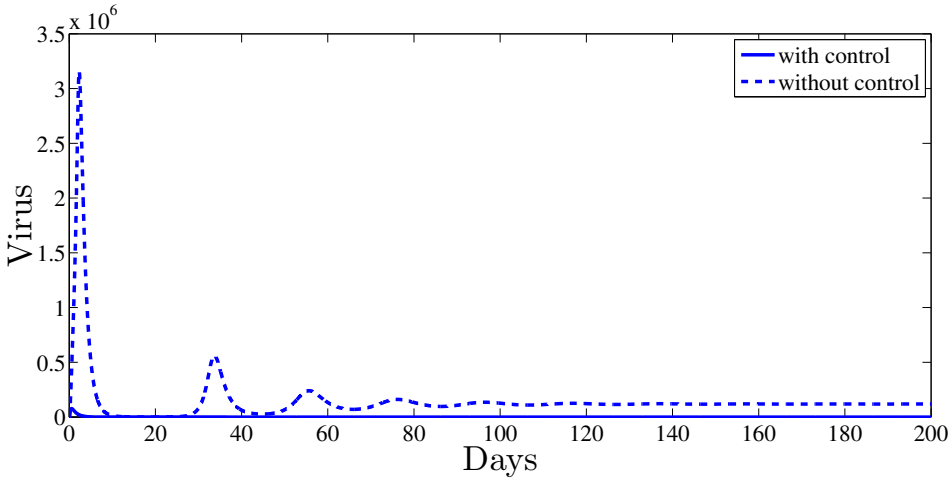

Figure 5: The effect of the control strategy on HBV

Figure 5 compares the levels of HBV (hepatitis B virus) under two conditions. Under the controlled condition, the viral load shows a significant decline or stabilization over time, indicating that the control strategy (such as antiviral therapy or immune modulation) effectively suppresses HBV replication. In contrast, the uncontrolled condition shows that the viral load remains persistently high or increases, signifying unchecked viral replication in the absence of intervention. The curve may fluctuate but remains elevated (e.g., near 2.5×10^6), highlighting the need for control measures. This stark contrast emphasizes the efficacy of the intervention, which is critical for managing infections and preventing liver damage.

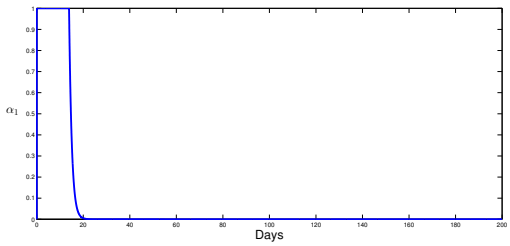

Figure 6: First control

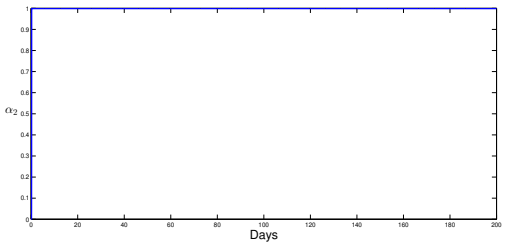

Figure 7: Second control

Figures 2, 3, 4, and 5 visually underscore the importance of control strategies in HBV management, with clear evidence of reduced viral load under treatment. Further details on

the specific intervention (such as drug type or dosage) would enhance the understanding of its impact.

Additionally, we observe in Figures 6 and 7 that the first control should be prioritized over the second within the first 20 days, based on the behavior of both controls. The prioritization of the first control within the first 20 days is consistent with the need to counteract rapid early viral replication. Early intervention via the first control is therefore critical to limit viral spread before secondary controls gain relevance.

5 Conclusion

In this paper, we have studied the HBV dynamics mathematically and numerically, as illustrated by system (2). We started by demonstrating the boundedness and positivity of the solutions, considering two control strategies. We calculated the BRN R_0, the steady states (both disease-free and endemic), and the critical therapy efficacy. Next, we applied optimal control techniques to minimize the proposed objective function. Numerically, we presented our results, confirming that control measures are essential for reducing viral load, which enhances disease management and helps prevent complications such as liver disease. In future work, we propose several extensions to improve the present paper. The current model does not account for several biologically relevant factors, including immune response, drug resistance, and spatial heterogeneity. To address these limitations and open new research avenues, we suggest exploring the development of a stochastic version of the model, a fractional-order formulation, multi-drug optimization approaches, or clinical validation studies.

Acknowledgements

The authors are grateful to their anonymous referees and the editor for their constructive comments.

Funding

This research received no external funding.

Conflicts of Interest

The authors declare no conflicts of interest.

References

[1] Ait Ichou, M., Bachraoui, M., Hattaf, K., and Yousfi, N. *Dynamics of a fractional optimal control HBV infection model with capsids and CTL immune response,* Math. Model. Comput. 10(1) (2023) 239–244.

[2] Bachraoui, M., Hattaf, K., and Yousfi, N. *Dynamics of a fractional order HBV infection model with capsids and CTL immune response,* Commun. Math. Biol. Neurosci., 2019 (2019), Article ID 6.

[3] Boudjaj, L., Naji, A., and Ghafrani, F. *Solving biharmonic equation as an optimal control problem using localized radial basis functions collocation method,* Eng. Anal. Bound. Elem. 107 (2019) 208–217.

[4] Churkin, A., Lewkiewicz, S., Reinharz, V., Dahari, H. and Barash, D. *Efficient methods for parameter estimation of ordinary and partial differential equation models of viral hepatitis kinetics,* Mathematics 8(9) (2020) 1483.

[5] Danane, J., Allali, K., and Hammouch, Z. *Mathematical analysis of a fractional differential model of HBV infection with antibody immune response,* Chaos Solitons Fractals 136 (2020) 109787.

[6] Danane, J., Meskaf, A., and Allali, K. *Optimal control of a delayed hepatitis B viral infection model with HBV DNA-containing capsids and CTL immune response,* Optim. Control Appl. Methods 39(3) (2018) 1262–1272.

[7] di Filippo Villa, D., and Navas, M.-C. *Vertical transmission of hepatitis B virus—An update.* Microorganisms 11(5) (2023) 1140.

[8] Elkaf, M., Meskaf, A., and Allali, K. *Mathematical Modeling of HBV Infection with DNA-Containing Capsids and Therapy,* In Nonlinear Dynamics and Complexity: Mathematical Modelling of Real-World Problems (pp. 413-427). Cham: Springer International Publishing, 2022.

[9] Foko, S. *Dynamical analysis of a general delayed HBV infection model with capsids and adaptive immune response in presence of exposed infected hepatocytes,* J. Math. Biol. 88(6) (2024) 75.

[10] Li, M., and Zu, J. *The review of differential equation models of HBV infection dynamics,* J. Virol. Methods 266 (2019) 103–113.

[11] Manna, K. *Global properties of an HBV infection model with HBV DNA-containing capsids and CTL immune response,* Int. J. Appl. Comput. Math. 3 (2017) 2323–2338.

[12] Manna, K., and Chakrabarty, S. P. *Chronic hepatitis B infection and HBV DNA-containing capsids: Modeling and analysis.* Commnu Nonlinear Sci. Numer. Simul. 22(1–3) (2015) 383–395.

[13] Meskaf, A., and Allali, K. *Optimal control of a delayed hepatitis B viral infection model with DNA-containing capsids and cure rate,* Trends in Biomathematics: Mathematical Modeling for Health, Harvesting, and Population Dynamics: Selected works presented at the BIOMAT Consortium Lectures, Morocco 2018 (2019): 23-33.

[14] Meskaf, A., Elkaf, M., and Aamoum, I. *Dynamics of HBV infection model with DNA-containing capsids, logistic hepatocyte growth and adaptive immune response,* Commun. Math. Biol. Neurosci. 2024 (2024), Article ID 58.

[15] Meskaf, A., Elkaf, M., and Allali, K. *Viral infection dynamics of HBV DNA-containing capsids with logistics growth and saturated rate,* Commun. Math. Biol. Neurosci., 2023 (2023), Article ID 7.

[16] Soriano, V., Moreno-Torres, V., Treviño, A., de Jesús, F., Corral, O., and de Mendoza, C. *Prospects for controlling hepatitis B globally.* Pathogens 13(4) (2024) 291.

[17] Sutradhar, R., and Dalal, D.C. *Re-cycling of DNA-containing capsids enhances hepatitis B virus infection,* arXiv preprint (2023) arXiv:2309.15665.

[18] Sutradhar, R., and Dalal, D.C. *Fractional-order models of hepatitis B virus infection with recycling effects of capsids,* Math. Methods Appl. Sci. 46(14) (2023) 15599–15625.

[19] World Health Organization. *Global health sector strategy on viral hepatitis 2016–2021: Towards ending viral hepatitis,* (2016).

[20] World Health Organization. *Advocacy brief: Strategic approaches to eliminate hepatitis B and C by 2030,* (2016).